

# Modeling of Kerr non-linear photonic components with mode expansion

Björn Maes ([bjorn.maes@intec.ugent.be](mailto:bjorn.maes@intec.ugent.be)), Peter Bienstman and Roel Baets

*Department of Information Technology, Ghent University – IMEC,  
St.-Pietersnieuwstraat 41, 9000 Ghent, Belgium*

**Abstract.** We present a numerical method to simulate the third order Kerr effect in wavelength scale dielectric structures. The intensity dependent refractive index is modeled by a spatial grid. By performing iterative linear eigenmode calculations, this index grid converges to the rigorous continuous-wave non-linear solution. Because the underlying eigenmode tool is bidirectional, feedback effects such as bistability can be calculated. We describe the influence of grid size, quantitative agreement with the literature and a photonic crystal switch.

**Keywords:** Mode expansion, Kerr effect

## 1. Introduction

The study of all-optical functions generates an interest in non-linear effects. A lot of attention is paid to the almost instantaneous Kerr effect, giving rise to an intensity dependent index change, allowing very fast processing. The strong confinement in advanced wavelength scale structures, such as photonic crystals or photonic wires, make it possible to use these weak effects with modest powers in integrated devices. Therefore there is a need for accurate and efficient methods to simulate these structures.

Among the available methods to model complex non-linear devices we mention the Finite-Difference Time-Domain method (FDTD) (Taflove, 1998) and the Beam Propagation Method (BPM) (Burzler et al., 1996). Each have their specific characteristics. FDTD e.g. models the full temporal evolution of a pulse-like excitation, but typically demands heavy calculations. BPM on the other hand propagates with small spatial steps along a certain direction and is most suitable in situations with fields propagating primarily in one direction, thus without multiple reflections.

Here we propose an alternative, building upon the eigenmode expansion method as implemented in (Bienstman and Baets, 2001). Mode expansion in general has a lot of attractive features such as rigorousness, efficiency, Perfectly Matched Layer (PML) boundary conditions, etc. Our non-linear extension enjoys these benefits and in addition, because



© 2003 Kluwer Academic Publishers. Printed in the Netherlands.

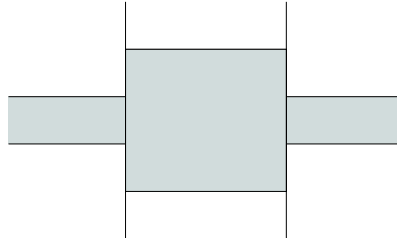


Figure 1. A simple structure with three sections.

we work in the frequency domain, we immediately get continuous-wave (CW) solutions. To get these solutions in FDTD we need to model long pulses, leading to long calculation times. Moreover, contrary to standard BPM, modes propagating in both directions are handled, thus it is possible to calculate non-linear feedback and interference effects, such as bistability.

In Section 2 we give a short overview of the linear mode expansion method and then present the non-linear extension. The method uses a grid and we will discuss the fineness thereof in Section 3 by a waveguide example. Then we will compare our results in Section 4 with a bistable grating structure from the literature. A more challenging device consisting of a photonic crystal cavity will be discussed in Section 5. After that a review of characteristics and a comparison with other methods is given in Section 6.

## 2. Method

The mode expansion method is now well established to model complex dielectric structures with linear materials. Before embarking upon non-linear problems it is helpful to review its basic principles.

### 2.1. LINEAR EIGENMODE EXPANSION

After defining a main propagation direction, one divides the structure in longitudinally invariant sections, as in Fig. 1. The field in such a section or slab can be described by a superposition of eigenmodes. The field profiles and propagation constants of these modes are derived from the transversal index profile. The electromagnetic fields in a section are in this way reduced to a vector of complex mode amplitudes:

$$(\mathbf{E}(\mathbf{r}), \mathbf{H}(\mathbf{r})) \longleftrightarrow \mathbf{A} = [A_i] \quad (1)$$

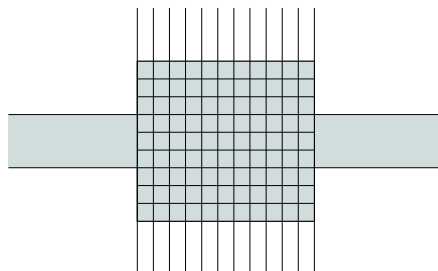


Figure 2. An example of spatial discretisation, the middle section is non-linear.

Different sections have different modes, but the mode-matching technique ensures the continuity of the tangential total field components and produces the reflection or transmission matrices. Combining these matrices with the propagation constants one can concatenate different sections to form a scattering matrix. With a chosen modal input excitation this algorithm gives the mode amplitudes and thus the fields throughout the structure.

## 2.2. EXTENSION FOR THE KERR EFFECT

If we want to simulate the Kerr effect, we have to take into account an intensity dependent refractive index:

$$n(\mathbf{r}) = n_0 + n_2 I(\mathbf{r}), \quad (2)$$

with  $n_0$  the linear index,  $n_2$  the Kerr coefficient and  $I$  the intensity. Because the intensity is spatially dependent, the refractive index is too, so we try to model this by dividing the non-linear section(s) in small rectangles, as in Fig. 2. Each rectangle will be assigned its refractive index during each iteration.

Because the intensity or index distribution is not known a priori, the method is iterative and proceeds as follows. We start from a certain index distribution, this can e.g. be the linear index or a previously calculated approximate solution. Using this index grid we perform a *linear* eigenmode calculation, yielding the fields in the structure. Using the intensities in the center of each rectangle we can update the refractive index distribution with Equation 2. If the new index distribution is equal to the old index distribution, within a certain tolerance, we have converged to a solution of the full non-linear problem. If not, we repeat the described procedure.

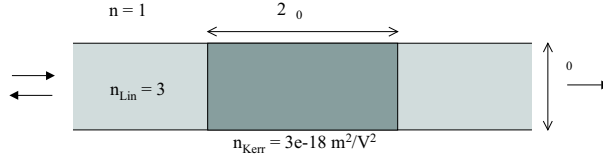


Figure 3. Waveguide with a non-linear section in a darker shade.

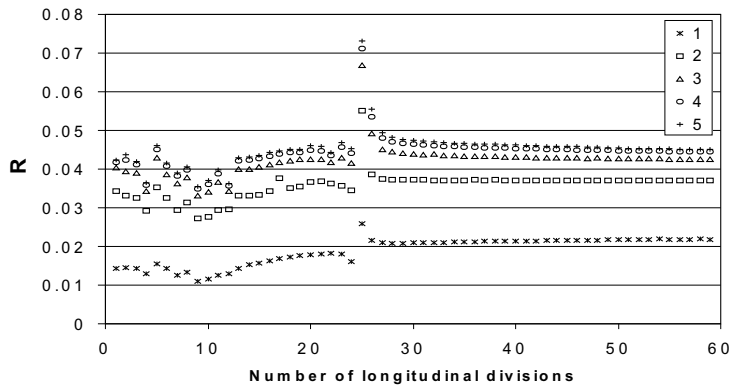


Figure 4. Magnitude of reflection coefficient of fundamental mode versus the number of longitudinal divisions, for different numbers of transversal divisions (inset).

### 3. Grid size

One intuitively assumes that the results should converge, as the grid becomes finer. We illustrate this by an example, a waveguide with a non-linear section, shown in Fig. 3. The multimode waveguide has a width  $\lambda$  and index 3.0, the cladding has index 1.0. A waveguide section of length  $2\lambda$  is considered with  $n_2 = 3 \times 10^{-18} \text{m}^2/\text{V}^2$ . For this test we use a high excitation, so that the maximum non-linear index change is about 0.2.

We varied the number of divisions in the longitudinal and transversal waveguide direction and calculated the reflection coefficient of the fundamental TE mode. As can be seen in Fig. 4, above a certain threshold the result remains invariant. More than 50 longitudinal and 4 transversal divisions give good results in this case. Of course the finer the grid, the longer the calculations take. Note that the spike at 25 longitudinal divisions is the result of a Bragg resonance between the rough sampling grid and the fundamental waveguide mode. As soon as the grid becomes finer, its  $k$ -vector does not agree anymore with the

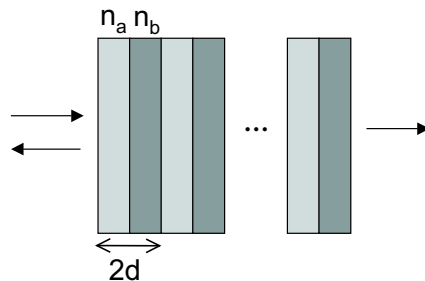


Figure 5. Grating with the non-linear sections in a darker shade.

propagation constant of the mode, and the sharp peak then disappears. As the required grid size is dependent on the unknown field structure, there is no simple relation of fineness versus desired accuracy. A solution is thus to study different grids for one input power, choose an accuracy threshold and then use this division to determine other related solutions. Another method is to use an adaptive grid, which we will discuss briefly in Section 6.

#### 4. Quantitative comparison

In order to validate the algorithm we have to compare our results with the literature. We present one example, a grating that exhibits bistability. This phenomenon, arising from feedback in combination with non-linearity, lies at the basis of many proposed all-optical components. The grating structure, depicted in Fig. 5, consists of 20 unit cells, each comprising two films with equal width  $d = 0.125\lambda$  and indexes respectively  $n_a = 1.5$  and  $n_b = 2.12$ . The first material is linear, while the second has a negative Kerr coefficient  $n_2 = -1$ . Note that for this example  $n = n_b\sqrt{1 + n_2 I}$ . The used frequency ( $\lambda = 1\mu\text{m}$ ) lies in the stopgap just above the bottom edge.

In Fig. 6 we plot the transmission of the grating, which agrees with Fig. 3 in (Chen and Mills, 1987). At low input power there is very low transmission, as we are working in the gap. Because of the non-linearity, at higher powers the system can switch to higher transmission states. There are even fields with unity transmission, which represent gap solitons.

With our method one starts with the linear index distribution and low input power. Gradually increasing the input power yields the low transmission curve. After the folding point of this curve, there is no longer a low transmission state and the solution switches to a higher

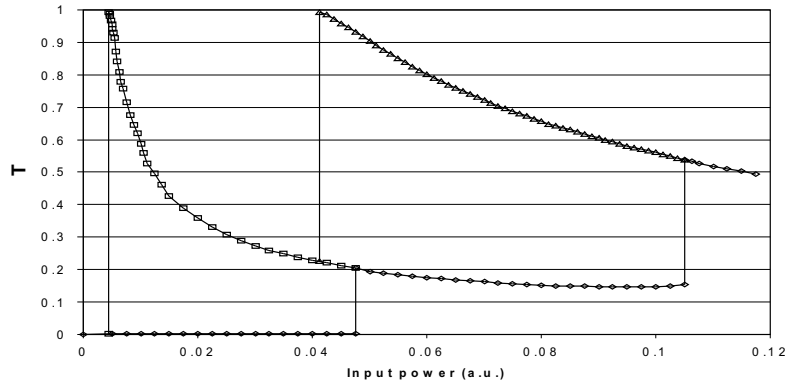


Figure 6. Transmission versus input power of the non-linear grating.

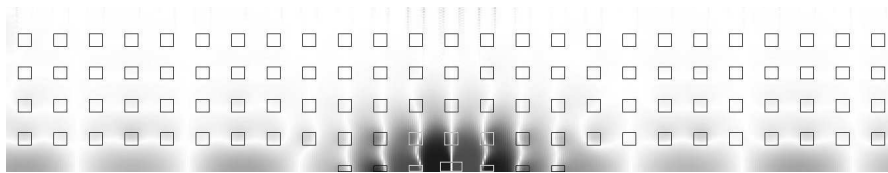


Figure 7. Structure of the photonic crystal device, the seven rods between the input and output waveguide are non-linear. The electric field of a completely transmitting resonant state is superimposed. The entire computational domain is shown.

non-linear solution. After finding one solution on an upper branch, we can then increase or decrease the power in steps to map the entire higher branch. If one would want to model these solutions with FDTD, the long input pulse would have to be preceded by a sufficiently strong short one, which complicates matters.

## 5. Photonic crystal device

Now we present calculation results on a bistable photonic crystal switch, shown in Fig. 7. This device has been described in (Soljagic *et al.*, 2002) and is particularly suited for our method. First of all it is obvious that the smaller the non-linear sections are, the more efficient our calculations become. In these calculations only the seven consecutive central rods are considered non-linear, a good approximation as they experience the strongest fields. Related to this, efficiency is improved because the linear sections before and after the non-linear rods have

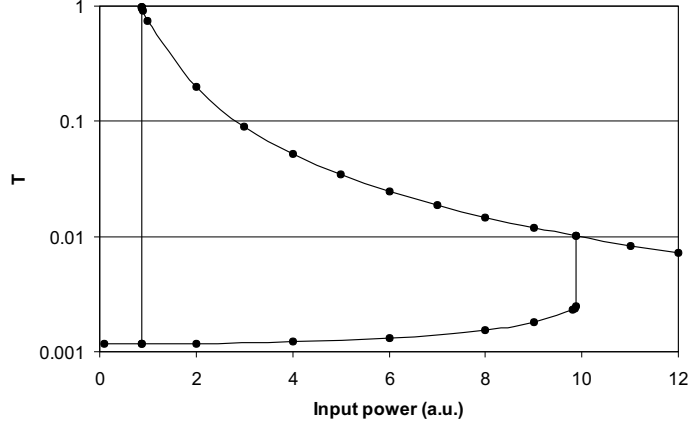


Figure 8. Transmission versus input power for the photonic crystal switch.

to be calculated only once, as they consist of linear materials, and therefore their transfer-matrix is power independent. In the longitudinal direction Fabry-Pérot effects are avoided by using non-reflecting semi-infinite repetitions of the photonic crystal waveguide period.

Let us briefly review the operation of the switch. The larger defect rod in the center forms a dipole-type cavity mode, which is coupled to input and output photonic crystal waveguides by tunneling effects through three normal-sized rods on either side. We operate on a frequency slightly below the linear resonance frequency of the cavity. So at low input almost all power reflects to the input waveguide. Increasing the input power changes the indices of the Kerr rods and the resonance frequency adjusts and shifts through the operating frequency. This means a stronger excitation of the cavity mode and leads to transmission of power to the output waveguide. Buildup in the high Q cavity makes the device even bistable.

This operation is clearly shown in our calculation results in Fig. 8. Here transmission is defined by dividing the flux of the longitudinal component of the Poynting vector at the end of the output waveguide with and without the seven center rods.

For the simulations we used a square lattice, with period  $0.6\mu\text{m}$ , of square rods with index 3.5 and side length  $0.24\mu\text{m}$  in air. The wavelength is  $1.87\mu\text{m}$ , which lies in the bandgap and close to the resonance wavelength  $1.8672\mu\text{m}$  formed by the defect rod with side length  $0.36\mu\text{m}$ . The non-linear rods have a realistic  $n_2 = 2 \times 10^{-19}\text{m}^2/\text{V}^2$ . Only sixty eigenmodes were used in these calculations.

## 6. Characteristics and comparison

This section brings together some characteristics and a comparison with other calculation methods.

An important issue is the number of iterations needed for convergence. Of course this is dependent on the desired accuracy and the deviation from a previous solution, but, as in the examples, with reasonable parameters convergence is mostly reached in about ten iterations. Some more difficult points however require another update equation, instead of Equation 2. These are e.g. points close to a folding bifurcation, the first solution on an upper branch or highly non-linear states, such as gap solitons. In these cases we use:

$$n'_{new} = (n_{new} + \alpha n_{old}) / (1 + \alpha), \quad \alpha \geq 0 \quad (3)$$

with  $n_{new}$  the index if we used the normal Kerr relation, Equation 2. With this weighted average we hold on longer to the previous index distribution  $n_{old}$ , the iterations are thus less abrupt. This prevents the solution from dropping back to more linear branches. Values of  $\alpha$  up to about thirty are sometimes necessary.

Another trait of our algorithm is that other types of Kerr-like non-linearities can easily be implemented. By adjusting Equation 2 we can e.g. model a saturable Kerr effect. Absorption has also been applied.

We note that the method is rigorous. There is no approximation in Maxwell's equations, so in the limit of an infinite number of modes and a very fine grid, the solutions are exact.

The bidirectional character of our mode solver gives us an advantage over unidirectional standard BPM programs. Concerning efficiency we already mentioned that linear sections need only one calculation and that we immediately get CW solutions, in contrast with FDTD. Moreover an adaptive grid can be implemented, which means we merge sections, if their non-linear index contrast is too small, or we refine them otherwise. In this way the calculation should find its optimal grid. Although adaptive gridding is very straightforward in our method, this is not the case with FDTD, as the latter requires special treatments on the boundaries between different grids.

## 7. Conclusions

We presented an extension to the eigenmode method which allows the modeling of 2D structures with Kerr materials. The efficiency of the linear bidirectional mode-expansion method, combined with the

smooth convergence to non-linear solutions, makes this method a fast and flexible alternative to FDTD and BPM.

### Acknowledgements

BM and PB acknowledge the Flemish Fund for Scientific Research (FWO-Vlaanderen) for a doctoral and postdoctoral fellowship, respectively. Parts of this work were performed in the context of the Belgian DWTC project IAP-Photon.

### References

- Bienstman, P. and R. Baets: 2001, 'Optical Modelling of Photonic Crystals and VCSELs Using Eigenmode Expansion and Perfectly Matched Layers'. *Opt. Quantum Electron.* **33**, 327–341. CAMFR simulation software is freely available from <http://camfr.sourceforge.net/>.
- Burzler, J. M., S. Hughes, and B. S. Wherrett: 1996, 'Split-Step Fourier Methods Applied to Model Nonlinear Refractive Effects in Optically Thick Media'. *Applied Physics B* **62**(4), 389–397.
- Chen, W. and D. L. Mills: 1987, 'Optical Response of Nonlinear Multilayer Structures: Bilayers and Superlattices'. *Phys. Rev. B* **36**, 6269–6278.
- Soljacic, M., M. Ibanescu, S. G. Johnson, Y. Fink, and J. D. Joannopoulos: 2002, 'Optimal Bistable Switching in Nonlinear Photonic Crystals'. *Phys. Rev. E* **66**, 055601.
- Taflove, A.: 1998, *Advances in Computational Electrodynamics: The Finite-Difference Time-Domain Method*. Boston, MA: Artech House.

